Estimation of aboveground biomass of arboreal species in the semi-arid region of Brazil using SAR (synthetic aperture radar) images postprint

Authors: Janisson B de JESUS, Tatiana M KUPLICH, Íkaro D de C BARRETO, Fernando L HILLEBRAND, Cristiano N da ROSA

Date: 2023-06-13T00:00:00+00:00

Abstract

The Caatinga biome is an important ecosystem in the semi-arid region of Brazil that has experienced significant degradation due to human activities and is currently undergoing desertification. Monitoring vegetation variation in the Caatinga has become essential for its sustainable development. Traditional methods for estimating aboveground biomass (AGB) are time-consuming and destructive, while remote sensing techniques using optical and radar imagery offer non-destructive alternatives. However, radar imaging remains novel for AGB estimation in this biome, where research is limited. This study aimed to use Sentinel-1 images to estimate AGB in the Caatinga biome of Sergipe State (northeastern Brazil) and identify influencing factors. Nineteen sample plots (30 m × 30 m) were selected, and stems of individuals with circumference at breast height (1.3 m above ground) $ 6.0cmweremeasuredtoestimateAGBusinganallometricequation.Sentinel − 1imagesfromthreeperiods(green, intermediate, anddry)wereusedtocapturephenologicalvariation.Allpre− processingandattributeextraction—includingco−polarizedVV(verticaltransmitandverticalreceive), cross− polarizedVH(verticaltransmitandhorizontalreceive), VH/VVbandratio, radarvegetationindex, dualpolariz = 0.73; r = 0.85; RMSE = 8.33 Mg/hm^2), followed by the green period (R^2 = 0.72; r = 0.85; RMSE = 8.40 Mg/hm^2). The contributing attri

Full Text

Preamble

Estimation of Aboveground Biomass of Arboreal Species in the Semi-Arid Region of Brazil Using SAR (Synthetic Aperture Radar) Images

Janisson B de JESUS[1], Tatiana M KUPLICH[2], Íkaro D de C BARRETO[3], Fernando L HILLEBRAND[4], Cristiano N da ROSA[5]

[1] Postgraduate Program in Remote Sensing, Federal University of Rio Grande do Sul, Campus Vale, Porto Alegre 91501970, Brazil
[2] National Institute for Space Research (INPE), COESU (Southern Spatial Coordination), Santa Maria 97105970, Brazil
[3] Postgraduate Program in Biometry and Applied Statistics, Rural Federal University of Pernambuco, Recife 52171900, Brazil
[4] Federal Institute of Education, Science and Technology of Rio Grande do Sul (IFRS), Campus Rolante, Rolante 95690000, Brazil
[5] Postgraduate Program in Remote Sensing, Polar and Climate Center, Federal University of Rio Grande do Sul, Porto Alegre 91501970, Brazil

Abstract: The Caatinga biome is an important ecosystem in the semi-arid region of Brazil that has experienced significant degradation due to human activities and is currently undergoing desertification. Monitoring vegetation variation in the Caatinga has become essential for its sustainable development. Traditional methods for estimating aboveground biomass (AGB) are time-consuming and destructive, while remote sensing techniques using optical and radar imagery offer non-destructive alternatives. However, radar imaging remains novel for AGB estimation in this biome, where research is limited. This study aimed to use Sentinel-1 images to estimate AGB in the Caatinga biome of Sergipe State (northeastern Brazil) and identify influencing factors. Nineteen sample plots (30 m × 30 m) were selected, and stems of individuals with circumference at breast height (1.3 m above ground) $ 6.0cmweremeasuredtoestimateAGBusinganallometricequation.Sentinel − 1imagesfromthreeperiods(green, intermediate, anddry)wereusedtocapturephenologicalvariation.Allpre− processingandattributeextraction—includingco−polarizedVV(verticaltransmitandverticalreceive), cross− polarizedVH(verticaltransmitandhorizontalreceive), VH/VVbandratio, radarvegetationindex, dualpolariz = 0.73; r = 0.85; RMSE = 8.33 Mg/hm^2), followed by the green period (R^2 = 0.72; r = 0.85; RMSE = 8.40 Mg/hm^2). The contributing attributes were VH/VV, DPSVI, H, α, and co-polarized VV for the green period, and cross-polarized VH for the intermediate period. The study demonstrated that Sentinel-1 images can estimate AGB in the Caatinga biome during green and intermediate phenological periods, as SAR attributes showed high correlation with AGB through multiple linear equations.

Keywords: Caatinga; tropical dry forest; coherent and incoherent attributes; C-band; Sentinel-1

1 Introduction

Drylands are important ecosystems covering over 40% of Earth's surface (Sörensen, 2007). These biomes occupy two-fifths of the planet, with semi-arid domains representing the largest portion of aridity zones (Bastin, 2017). In South America, among the three existing semi-arid extensions, the Caatinga biome stands out as Brazil's representative climate zone, characterized by

high annual average temperatures, high spatial and temporal precipitation variability, and strong evaporation (Nóbrega et al., 2016). According to the Brazilian Ministry of Environment (MMA, 2021), this biome occupies approximately 11% of the country's territory across ten states.

Ecological, social, and economic issues threaten this biome, as Brazil's semi-arid lands undergo desertification exacerbated by deforestation and land abandonment from agriculture, grazing, and firewood harvesting. These activities increase soil degradation and reduce precipitation, making the region more vulnerable to drought (Althoff et al., 2016; Salvatierra et al., 2017; Vendruscolo et al., 2020). Researchers have increasingly focused on this process and its consequences in Brazil (Vieira et al., 2015; Tomasella et al., 2018; Bezerra et al., 2020; Vieira et al., 2020, 2021; Barbosa Neto et al., 2021).

As Caatinga area decreases, quantifying vegetation biomass and verifying its loss becomes crucial for understanding carbon release and storage (Menezes et al., 2021). While field measurements are commonly used for AGB evaluation in the Caatinga (Souza et al., 2019; Castanho et al., 2020a; Maia et al., 2020; Menezes et al., 2021; Oliveira et al., 2022), traditional forest inventory methods, though accurate, are laborious and time-consuming. Therefore, developing indirect biomass estimation strategies using remote sensing is essential (Baccini et al., 2004; Akhtar et al., 2020). Various remote sensors based on different characteristics estimate vegetation AGB, with primary data sources being optical, LiDAR (light detection and ranging), and radar (Kumar et al., 2015).

Despite limited studies estimating AGB through traditional methods in different Caatinga vegetation types, remote sensing applications remain scarce. Some research exists at local (Lima Júnior et al., 2014; Fernandes, 2018; Silveira et al., 2020; Oliveira et al., 2021) and global scales using optical orbital sensors and LiDAR (Saatchi et al., 2011; Baccini et al., 2012). However, active synthetic aperture radar (SAR) sensors have not been applied in this biome.

SAR imaging offers specific advantages over optical imaging for biomass estimation in savanna-like regions such as the Caatinga. Longer microwave wavelengths experience fewer cloud effects, which is vital in tropical environments with near-constant cloud cover. Additionally, microwaves directly interact with vegetation structure by penetrating the canopy (Kumar et al., 2015). Sentinel-1, a recently launched orbital radar by the European Space Agency (ESA), operates at C-band wavelength and provides free imagery (Nuthammachot et al., 2022). Its data have been used in forest AGB estimation studies (Forkuor et al., 2020; Mayamanikandan et al., 2020; Safari and Sohrabi, 2020; Ghosh and Behera, 2021; Malhi et al., 2021; Vaghela et al., 2021).

Given Sentinel-1's characteristics, its data should allow significant interaction with arboreal Caatinga biomass, considering microwave pulse penetration into the canopy and interaction with structural vegetation characteristics, particularly during periods of lower leaf cover. This study therefore evaluated Sentinel-1 SAR C-band images to estimate aerial biomass of the Caatinga biome across

three phenological periods (green, intermediate, and dry), identifying which period and attributes correlate most strongly with AGB.

2.1 Study Area

This study was conducted near the Grota do Angico Natural Monument Conservation Unit in the municipalities of Canindé de São Francisco and Poço Redondo, Sergipe State [FIGURE:1], located in Brazil's semi-arid region according to the National Institute of the Semi-Arid (INSA, 2019). The local climate is classified as BSh (hot arid steppe) by Köppen classification, with annual precipitation below 700 mm and average temperatures of 24°C–26°C (Alvares et al., 2014). This region has monthly aridity indices indicating high desertification risk (Jesus et al., 2019a) and is designated as a desertification area by the National Forest Inventory of the Brazilian Forest Service (MMA, 2018).

Vegetation is characteristic of the Caatinga biome, composed of deciduous thorny trees and shrubs typical of semi-arid to arid climates (Veloso et al., 1991), with dense forest remnants of hyper-xerophytic Caatinga (Ribeiro and Mello, 2007) occurring across different physiographic characteristics (Jesus et al., 2019b). This plant typology exhibits high phenological variation in leaf cover due to rainfall variability (Jesus et al., 2021) and is categorized as a tropical dry forest (FAO, 2012). Soils are Luvisolos and Planossolos (Embrapa, 2011), with dissected relief on hills, tabular interflows, and a pediplan surface in the Sertão Pediplano (SEMARH, 2012).

2.2 Methodological Flowchart

The study comprised two stages linking field activities and Sentinel-1 image analysis

. The first stage involved forest inventory of arboreal Caatinga species to estimate biomass from densitometric calculations. A pilot inventory with six plots tested data collection feasibility and area selection for sample plot implementation, followed by measurement of 12 additional plots to complete the inventory. The second stage involved acquiring and pre-processing Sentinel-1 images, concluding with attribute generation and extraction for each field-sampled unit for statistical analysis of field and satellite data.

2.3 Obtaining Field Data and Estimating Arboreal Aboveground Biomass

Fieldwork was conducted in two phases as indicated in the methodological flowchart

. The pilot inventory occurred December 16–20, 2018, and the final inventory from September 8–15, 2019. Timing was selected based on Caatinga phenology

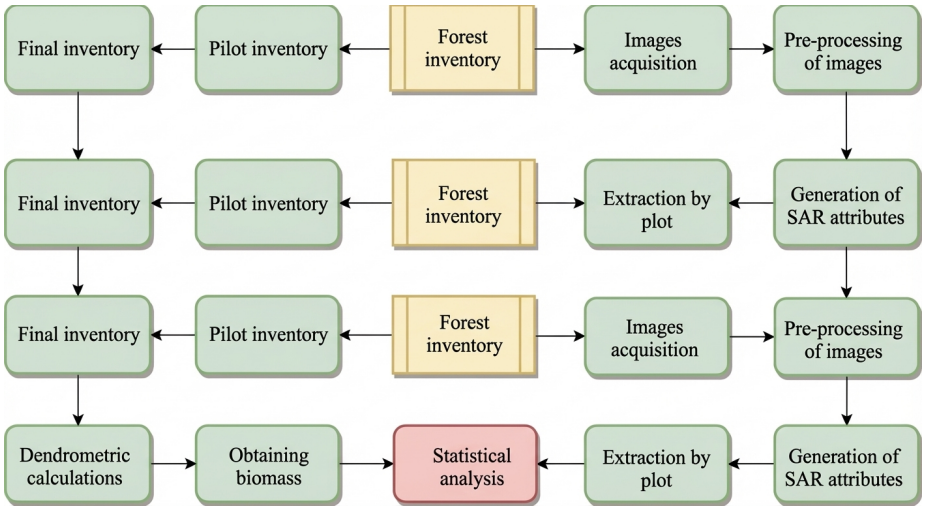

Figure 1: Figure 2

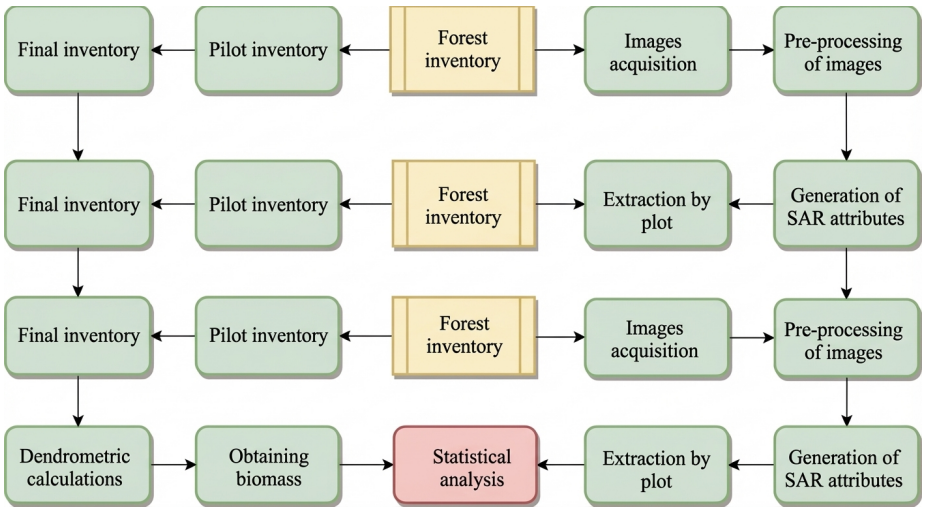

Figure 2: Figure 2

(Jesus et al., 2021) to conduct dendrometric surveys during intermediate phenological conditions and periods close to both rainy and dry seasons. Given the region's high rainfall variability, AGB data for the intermediate period could be associated with green and dry periods near inventory dates.

Plot locations were selected based on vegetation conservation status variation (from degraded to conserved) resulting from human activity interference. Nineteen plots were installed near the Grota do Angico conservation unit [FIGURE:1] to maximize variation in biomass, density, composition, and individual distribution. Taxonomic identification, classification, and nomenclature are detailed in Jesus et al. (2022). Dominant tree species included *Cenostigma pyramidale* (Tul.) Gagnon & G. P. Lewis (1,240 individuals, 51.8% of total), followed by *Aspidosperma pyrifolium* Mart. & Zucc. (542 individuals), *Jatropha mollissima* (Pohl) Baill. (150 individuals), *Mimosa tenuiflora* (Willd.) Poir. (120 individuals), and *Piptadenia retusa* P. G. Ribeiro, Seigler & Ebinger (109 individuals).

Each plot measured 30 m × 30 m (900 m^2), totaling 16,200 m^2 of inventoried area. Plots were georeferenced using a Garmin GPSMap C/A GNSS receiver. Within each sampling unit, all living and dead individuals with circumference at breast height (CBH) $ $6.0 cm (1.3 m from ground) were recorded according to the Caatinga Forest Management Network (2005). CBH was measured with a tape and total height (H) with a telescopic rod. CBH values were converted to diameter at breast height (DBH), a widely used dendrometric measure in Caatinga research (Lima et al., 2018; Lopes et al., 2020; Souza et al., 2020; Menezes et al., 2021; Pereira et al., 2021). Individual tree AGB was calculated using the allometric equation from Sampaio and Silva (2005): $0.173 \times (\mathrm{DBH})^{2 \cdot 295}$, $R^2 = 0.9184$. Plot-level biomass (kg) was converted to megagrams per hectare (Mg/hm^2).

2.4 Acquisition, Pre-processing, and Retrieval of Sentinel-1 Data

Image acquisition dates were selected based on Caatinga leaf cover state using normalized difference vegetation index (NDVI) variation. Periods with high, intermediate, and low NDVI values representing green, intermediate, and dry vegetation conditions were selected using Sentinel-1 images acquired on: 2019/01/18–2019/09/03 for the green period, 2018/08/15–2019/10/09 for the intermediate period, and 2018/10/26–2019/11/26 for the dry period [FIGURE:3].

NDVI values were obtained through pre-filtering in dense arboreal Caatinga using the SATVeg web-based tool. MODIS NDVI has 250 m × 250 m spatial resolution with 16-day temporal composition (Embrapa, 2018). Monthly precipitation data were acquired from the Canindé de São Francisco meteorological station via the Agricultural Development Company of Sergipe website (Emdagro, 2020).

Sentinel-1 images were acquired from the European Space Agency website (ESA, 2020a) during the two-year study period. Images were in descending mode, orbit

82, interferometric wide mode, with 250 km swath width, 29.1°–46.0° incidence angle range, 3 sub-swaths, $±$0.6° azimuth steering angle, and dual/single polarization. Ground range detected (GRD) high-resolution and single look complex (SLC) formats were used, with pixel spacing of 10.0 m × 10.0 m and 2.3 m × 14.1 m, 5$×1*and*1×$1 looks, equivalent number of looks of 4.4 and 1.0, both level 1, in VV (vertical transmit and vertical receive) and VH (vertical transmit and horizontal receive) polarizations.

GRD images were pre-processed following Filipponi (2019) to match SLC pixel dimensions. Multilooking was applied with four looks (1 in azimuth, 4 in range), and images were subset to expedite processing. A gamma 5$×5*filterwasappliedtoGRDimages*,*whilepolarimetricfilterswereappliedtoSLCimages*,*whichshowedstron*
1*byNasirzadehdizajietal.*(2019),*andthedualpolarizationSARvegetationindex*(*DPSVI*)*proposedbyPeriasam*
attributes were obtained from SLC images. All image processing and attribute extraction (VH, VV, VH/VV, RVI, DPSVI, H, and α) were performed using SNAP v.8.0 (ESA, 2020b), with plot sampling in each band using QGIS v.3.18.

2.5 Statistical Analysis

SAR attributes were individually evaluated using simple linear regression to assess their contribution to AGB estimation for each period. Hypothesis testing used P-value analysis at 5% significance level, with coefficient of determination (R^2) and root mean squared error (RMSE) calculated for each linear equation. Multiple linear regressions were then calculated using all possible attribute combinations, selecting the best biomass estimation equation for each period based on parsimony principles, considering R^2, correlation coefficient (r), and RMSE. Relationships between observed and estimated data and residual error distributions were graphed. Statistical analysis was performed using R Core Team 2021 software v.4.1.0.

3 Results

AGB distribution across all plots showed similar patterns, with most individuals having low values and small peaks around 50.00 kg [FIGURE:4a]. This increase varied quantitatively between plots: plots 10, 11, and 18 had more individuals with lower AGB values, while plot 17 had more high-AGB individuals. Generally, each plot had standout individuals, but plots 7, 9, 14, 16, and 17 contained individuals with much higher AGB than other plots. Plot 14, despite having only one individual, recorded the highest biomass (1,875.66 kg). Conversely, plot 11 had low AGB values with just two arboreal representatives and the smallest calculated AGB per plot among those with registered individuals. Plot 19 had no arboreal representatives (0.00 kg AGB). Total biomass varied between plots: plots 10, 18, 12, 8, 17, and 4 had 10.00–20.00 Mg/hm^2; plots 14 and 7 had 20.84 and 21.60 Mg/hm^2, respectively; plots 13 and 1 had 32.80 and 39.83 Mg/hm^2, respectively. Plots 9, 16, 15, 6, 2, 3, and 5 had higher AGB values, with plot 5 recording the highest at 46.63 Mg/hm^2 [FIGURE:4b].

Hypothesis test results from P-value statistical analysis showed no SAR attribute significantly explained AGB in simple linear regression during the green period. In the other two periods, two attributes showed significant differences at the 5% level. VH polarization stood out in intermediate and dry periods (P = 0.030 and 0.034, respectively), while the lowest P-values were observed for α in the intermediate period (0.022) and VV polarization in the dry period (0.010).

Individual SAR attributes showed weak relationships with estimated biomass, evidenced by low R^2 and high RMSE across all periods [FIGURE:5]. VH polarization performed best with highest R^2 for green vegetation (0.161), a period that generally showed the lowest coefficient values. VH was also second-best for intermediate (0.238) and dry (0.248) periods. The highest R^2 overall was VV-dryness (0.330) and α-intermediate (0.269). Attributes with best R^2 generally had highest RMSE, except α-intermediate, which had the lowest RMSE (14.39 Mg/hm^2) among all analyzed attributes.

Multiple linear regression revealed DPSVI was present in all three period equations . In the dry period, the best attribute combination included only DPSVI and cross-polarization (VH). Green and intermediate period equations differed only between VV and VH polarizations, respectively, highlighting the importance of VH/VV, H, α, and the vegetation index for AGB estimation.

Multiple regression equations achieved substantially higher R^2 values (0.720 green, 0.730 intermediate, 0.550 dry) than simple regressions, establishing high positive correlations between observed and estimated variables (r = 0.85 for green and intermediate, r = 0.74 for dry). While only the intermediate period regression estimated 50.00 Mg/hm^2 (plot 5), data were distributed closer to the regression line compared to green and dry periods [FIGURE:6].

Residual analysis by RMSE showed intermediate period AGB estimation error (8.33 Mg/hm^2) was lower than green (8.40 Mg/hm^2) and dry (10.65 Mg/hm^2) periods. Residual error distribution by plot [FIGURE:6] showed error scale variation following RMSE increasing order: 28.20 Mg/hm^2 amplitude for intermediate, 30.50 Mg/hm^2 for green, and 39.57 Mg/hm^2 for dry. Plots 4, 15, and 16 showed greater discrepancies between estimated and observed AGB, with plot 9 also highlighted for green and dry periods, and plot 11 for dry period.

4 Discussion

Calculated AGB showed most arboreal individuals had low values in the studied Caatinga biome, indicating numerous individuals with smaller dendrometric dimensions (primarily diameters), characteristic of regenerating forest communities and verified in other Caatinga inventories (Lima et al., 2018; Lopes et al., 2020; Nascimento Neto et al., 2020). Diameter influence on individual AGB caused varying biomass responses between plots, as seen comparing plots 11 and 14, which had 2 and 1 individuals but vastly different AGB (0.17 vs. 20.84 Mg/hm^2). This influence also appeared in AGB variation relative to individual

numbers, where plots 7, 8, 9, and 17, despite fewer individuals, were not among the lowest biomass plots, demonstrating sampling unit composition variability. However, plots with most tree representatives (2, 3, 5, 6, and 15) had highest AGB, except plot 13 with 228 individuals but only 32.80 Mg/hm^2 due to small diameters. Thus, AGB variation also reflects different vegetation phytophysiognomies and conservation statuses, as verified by Castanho et al. (2020b) and Menezes et al. (2021).

Statistical relationships from linear regression between plot-level AGB and individual SAR attributes showed slight response variation, as most interactions for evaluated phenological periods were non-significant at 5% level, indicating individual attributes do not influence AGB. However, four responses impacted AGB equations, with VH polarization being the only statistically significant attribute in two periods (intermediate and dry), demonstrating variation between SAR attribute responses and vegetation phenological period, and showing AGB estimates depend on image acquisition timing (Nguyen et al., 2016). Despite these interactions, overall relationships between SAR attributes and AGB were weak, as evidenced by low R^2 and high RMSE.

Among polarized data, VH polarization achieved highest R^2 for green vegetation (0.161) and was second-most accurate for intermediate (0.248) and dry (0.238) periods, showing importance of this polarization's interaction across Caatinga seasonalities. However, VV polarization achieved highest R^2 overall (0.330) in the dry period, indicating greater response to leafless vegetation, possibly suggesting this polarization's backscatter intensity is more sensitive to AGB in dry season than rainy season (Nguyen et al., 2016). Malhi et al. (2021) also found VV polarization superior (r = 0.74) to cross-polarization (r = 0.05) for Sentinel-1 in India's dense tropical forest. Different results were reported by Navarro et al. (2019) with R^2 = 0.900 in Senegal mangrove forest with AGB <35.00 Mg/hm^2; Safari and Sohrabi (2020) found better AGB correlation in Iran's Zagros oak forests; and Nuthammachot et al. (2022) indicated cross-polarization may be more AGB-sensitive than co-polarization.

VH polarization's contribution to AGB estimation in green and intermediate periods, compared to VV and HH, may result from lower soil moisture influence (Huang et al., 2018) and greater volumetric dispersion from high canopy density (Laurin et al., 2018). This polarization was also important in multiple linear equations for intermediate and dry periods, possibly due to interaction with the Caatinga's characteristic high branching density, producing more significant volumetric scattering expected from cross-polarization.

Comparing accuracy with other dryland AGB estimation studies using Sentinel-1 , only Forkuor et al. (2020) in African savanna reported higher R^2 (0.760) than this study (0.730), even using only backscatter coefficients. David et al. (2022), also in African savanna using backscatter coefficients, obtained lower R^2 (0.580), demonstrating radar response variation. Jesus et al. (2023) in the same Caatinga biome using H and α data also showed lower accuracy (0.320), indicating these data alone provide poor relationships. Other dry environment studies showed

lower R^2 values: Bao et al. (2019) used backscatter and texture data, achieving best accuracy (0.500) with VH polarization in China's Hulun Buir grassland; Pötzschner et al. (2022) reported $R^2 = 0.690$ using backscatter in South America's dry Chaco ecoregion.

Cross-polarization was also highlighted in L-band studies. Mitchard et al. (2009) found HV polarization outperformed HH ($R^2 = 0.730$ vs. 0.550) using ALOS PALSAR across African savanna regions. Nguyen et al. (2016) found HV polarization explained 54% of biomass variation in Vietnam's deciduous tropical forest using ALOS PALSAR-2. Wingate et al. (2018) achieved $R^2 = 0.740$ estimating AGB in Namibian savanna using PALSAR and PALSAR-2 with logarithmic models. Braun et al. (2018) estimated AGB in low-biomass savanna ecosystems, achieving best response ($R^2 = 0.520$) using ALOS PALSAR, Envisat, and SSM/I data with nonlinear regression, though noting linear, logarithmic, or multivariate techniques could also perform well depending on AGB-backscatter relationships.

This was verified in the dry period, where VH polarization combined with DPSVI achieved $R^2 = 0.550$, higher than all individual attributes across all periods. However, adding other attributes did not improve dry period accuracy. Forkuor et al. (2020) reported similar results in savanna AGB estimation, where more SAR variables (VV, VH, VH-VV, VH+VV) did not improve accuracy ($R^2 = 0.660$), with better results using only VH and VV ($R^2 = 0.760$). For green and intermediate periods, using five related attributes significantly increased accuracy with high R^2 and low RMSE.

Among multiple regression attributes, DPSVI was notable for appearing in all three period models. Periasamy (2018) also found DPSVI relevant for AGB estimation in Tamil Nadu, India, with forest and barren landscapes in both dry ($R^2 = 0.730$) and rainy seasons ($R^2 = 0.700$) through simple linear regression, demonstrating this index's vegetation biomass relationship.

The band ratio appeared in multiple linear equations for green and intermediate periods, contrasting with Laurin et al. (2018), who reported stronger Sentinel-1 band ratio relationships under deciduous vegetation conditions. Band ratio may be sensitive to SAR interaction with small branches more exposed without canopy cover, contributing to AGB given high branch density. This difference may be explained by their study area comprising broadleaf forests with high AGB, unlike Caatinga physiognomy.

Coherent attributes (H and α) from Sentinel-1 images were also relevant for Caatinga AGB estimation in green and intermediate periods, indicating that scattering type and randomness information from microwave phase data contributes to multiple relationships with the estimated variable, which is unavailable in incoherent backscatter coefficient data. Cartus et al. (2021) studied semi-arid forests in California's Sierra National Forest, and Ghosh and Behera (2021) verified coherent Sentinel-1 data importance in modeling AGB estimates for India's eastern coast tropical mangrove forests. Huang et al. (2018) simi-

larly used PALSAR-2 L-band polarimetric decomposition information, such as alpha angle, to generate more accurate AGB models in northern New England's eastern temperate forest.

Despite good observed-estimated AGB relationships, it is important to note that other components present in Caatinga sample plots may have caused estimation errors, including herbaceous plants (*Croton heliotropiifolius* Kunth, *Helleborus foetidus* L., *Senna obtusifolia* (L.) H.S.Irwin & Barneby), Cactaceae (*Cereus jamacaru* DC. and *Xiquexique gounellei* (F.A.C.Weber) Lavor & Calvente), and exposed stones characteristic of regional soils. These elements may have influenced radar signal interaction, as microwaves interact with all plot components, resulting in Sentinel-1 image pixels affected by non-AGB components.

5 Conclusions

This study demonstrated that combining polarized attributes with polarimetric decomposition data from Sentinel-1 images allowed high correlation with arboreal Caatinga AGB estimates using multiple linear regression. Isolated attributes, however, did not produce good relationships between estimated and observed variables under evaluated vegetation conditions. The intermediate phenological condition produced the best biomass estimation results, followed by the green period, differing only by VH versus VV attribute composition in the multiple linear equations. Despite strong drought conditions (dry period) showing lowest R^2 among multiple regressions, its value exceeded all individual attributes across all Caatinga conditions.

Sentinel-1 C-band images can therefore estimate arboreal Caatinga AGB, showing high correlation between attributes and the estimated variable. Sentinel-1 also provides an alternative to optical imagery given cloud cover acquisition challenges. However, although this study captured maximum local vegetation variation, the Caatinga biome contains diverse phytophysiognomies requiring AGB capacity evaluation for each typology and appropriate allometric equations. Different image pre-processing approaches and additional radar data may also generate different AGB correlation results.

Acknowledgements: The authors thank the National Council for Scientific and Technological Development (CNPq) and the Coordination of Superior Level Staff Improvement, Brazil (CAPES) for supporting this research.

References

Akhtar A M, Qazi W A, Ahmad S R, et al. 2020. Integration of high-resolution optical and SAR satellite remote sensing datasets for aboveground biomass estimation in subtropical pine forest, Pakistan. *Environmental Monitoring and Assessment*, 192.

Althoff T D, Menezes R S C, Carvalho A L, et al. 2016. Climate change impacts on the sustainability of the firewood harvest and vegetation and soil carbon

stocks in a tropical dry forest in Santa Teresinha Municipality, Northeast Brazil. *Forest Ecology and Management*, 360: 367–375.

Alvares C A, Stape J L, Sentelhas P C, et al. 2014. Köppen's climate classification map for Brazil. *Meteorologische Zeitschrift*, 22(6): 711–728.

Baccini A, Friedl M A, Woodcock C E, et al. 2004. Forest biomass estimation over regional scales using multisource data. *Geophysical Research Letters*, 31(10): L10501, doi: 10.1029/2004GL019782.

Baccini A, Goetz S J, Walker W S, et al. 2012. Estimated carbon dioxide emissions from tropical deforestation improved by carbon-density maps. *Nature Climate Change*, 2: 182–185.

Bao N, Li W, Gu X, et al. 2019. Biomass estimation for semiarid vegetation and mine rehabilitation using Worldview-3 and Sentinel-1 SAR imagery. *Remote Sensing*, 11(23): 2855, doi: 10.3390/rs11232855.

Barbosa Neto M V B, Araújo M S B, Araújo Filho J C, et al. 2021. Rill and sheet soil erosion estimation in an area undergoing desertification in the Brazilian semi-arid region. *Modeling Earth Systems and Environment*, 7: 1183–1191.

Bastin J F, Berrahmouni N, Grainger A, et al. 2017. The extent of forest in dryland biomes. *Science*, 356(6338): 635–638.

Bezerra F G S, Aguiar A P D, Alvalá R C S, et al. 2020. Analysis of areas undergoing desertification, using EVI2 multi-temporal data based on MODIS imagery as indicator. *Ecological Indicators*, 117: 106579, doi: 10.1016/j.ecolind.2020.106579.

Braun A, Wagner J, Hochschild V. 2018. Above-ground biomass estimates based on active and passive microwave sensor imagery in low-biomass savanna ecosystems. *Journal of Applied Remote Sensing*, 12(4): 046027, doi: 10.1117/1.JRS.12.046027.

Cartus O, Santoro M, Wegmüller U, et al. 2021. Sentinel-1 coherence for mapping above-ground biomass in semiarid forest areas. *IEEE Geoscience and Remote Sensing Letters*, 19: 4012805, doi: 10.1109/LGRS.2021.4012805.

Castanho A D A, Coe M T, Brando P, et al. 2020a. Potential shifts in the above-ground biomass and physiognomy of a seasonally dry tropical forest in a changing climate. *Environmental Research Letters*, 15(3): 034053, doi: 10.1088/1748-9326/ab7394.

Castanho A D A, Coe M T, Andrade E M, et al. 2020b. A close look at above ground biomass of a large and heterogeneous seasonally dry tropical forest–Caatinga in North East of Brazil. *Annals of the Brazilian Academy of Sciences*, 92(1): e20190282, doi: 10.1590/0001-3765202020190282.

David R M, Rosser N J, Donoghue D N M. 2022. Improving above ground biomass estimates of Southern Africa dryland forests by combining Sentinel-1

SAR and Sentinel-2 multispectral imagery. *Remote Sensing of Environment*, 282: 113232, doi: 10.1016/j.rse.2022.113232.

Embrapa (Brazilian Agricultural Research Corporation). 2011. Brazilian system of soil classification. Brazilian soils. Soil map of Brazil. [2021-01-11]. https://wwwembrapabr/tema-solos-brasileiros/solos-do-brasil. (in Portuguese)

Embrapa (Brazilian Agricultural Research Corporation). 2018. SATVeg. Vegetation Temporal Analysis System. [2021-01-10]. https://wwwsatvegcnptiaembrapabr/satveg/loginhtml. (in Portuguese)

Emdagro. 2020. Agricultural Development Company of Sergipe. Statistic Agriculture. Rainfall. [2021-01-10]. https://wwwemdagrosegovbr/pluviosidade/. (in Portuguese)

ESA (European Space Agency). 2020a. Copernicus. Open Access Hub. [2021-10-14]. https://scihubcopernicuseu/dhus/#/home.

ESA (European Space Agency). 2020b. SNAP. [2021-11-18]. https://stepesaint/main/download/snap-download/.

FAO (Food and Agriculture Organization of the United Nations). 2012. Global Ecological Zones for FAO Forest Reporting: 2010 Update. Rome: Forest Resources Assessment Working, 52.

Fernandes M R M. 2018. Estimation of basal area, volume and biomass in a fragment of Caatinga dense hyperxerophile in the high Sergipe sertão based on data MSI/Sentinel-2. PhD Dissertation. Espírito Santo: Federal University of Espírito Santo. (in Portuguese)

Filipponi F. 2019. Sentinel-1 GRD preprocessing workflow. *Proceedings*, 18(1): 11, doi: 10.3390/ECRS-3-06201.

Forkuor G, Zoungrana J-B B, Dimobe K, et al. 2020. Above-ground biomass mapping in West African dryland forest using Sentinel-1 and 2 datasets–A case study. *Remote Sensing of Environment*, 236: 111496, doi: 10.1016/j.rse.2019.111496.

Ghosh S M, Behera M D. 2021. Aboveground biomass estimates of tropical mangrove forest using Sentinel-1 SAR coherence data–the superiority of deep learning over a semi-empirical model. *Computers & Geosciences*, 150: 104737, doi: 10.1016/j.cageo.2021.104737.

Huang X, Ziniti B, Torbick N, et al. 2018. Assessment of forest above ground biomass estimation using multi-temporal C-band Sentinel-1 and polarimetric L-band PALSAR-2 data. *Remote Sensing*, 10(9): 1424, doi: 10.3390/rs10091424.

Institute. 2019. Global Network of Dryland Research (Semi Arid National Institute). [2021-03-22]. https://www.gndri.org/institutions/semi-arid-national-institute-instituto-nacional-do-semiarido-insa/. (in Portuguese)

Jesus J B, Souza B B, Oliveira A M S, et al. 2019a. Aridity index and climatic risk of desertification in the semi-arid state of Sergipe. *Brazilian Journal of Climatology*, 24: 214–227.

Jesus J B, Ribeiro M M, Kuplich T M, et al. 2019b. Statistical analysis of the spatial relationship of Caatinga and physiographic factors through remote data. *Revista Floresta*, 49(4): 755–762.

Jesus J B, Kuplich T M, Barreto I D C, et al. 2021. Temporal and phenological profiles of open and dense Caatinga using remote sensing: Response to precipitation and its irregularities. *Journal of Forestry Research*, 32: 1067–1076.

Jesus J B, Oliveira D G, Araújo W S, et al. 2022. Influence of anthropization on the floristic composition and phytosociology of the Caatinga susceptible to desertification in the state of Sergipe, Brazil. *Tropical Ecology*, 63: 398–408.

Jesus J B, Kuplich T M, Barreto I D C, et al. 2023. Dual polarimetric decomposition in Sentinel-1 images to estimate aboveground biomass of arboreal caatinga. *Remote Sensing Applications: Society and Environment*, 29: 100897, doi: 10.1016/j.rsase.2022.100897.

Kim Y, van Zyl J. 2004. Vegetation effects on soil moisture estimation. In: *Proceedings of the International Geoscience and Remote Sensing Symposium*. IEEE International Geoscience and Remote Sensing Symposium, Anchorage: Institute of Electrical and Electronics Engineers, 800–802.

Kumar L, Sinha P, Taylor S, et al. 2015. Review of the use of remote sensing for biomass estimation to support renewable energy generation. *Journal of Applied Remote Sensing*, 9(1): 097696, doi: 10.1117/1.JRS.9.097696.

Laurin G V, Balling J, Corona P, et al. 2018. Above-ground biomass prediction by Sentinel-1 multitemporal data in central Italy integration of ALOS2 and Sentinel-2 data. *Journal of Applied Remote Sensing*, 12(1): 016008, doi: 10.1117/1.JRS.12.016008.

Lima Júnior C, Accioly L J O, Giongo V, et al. 2014. Estimation of "Caatinga" woody biomass using allometric equations and vegetation index. *Scientia Forestalis*, 42(102): 289–298. (in Portuguese)

Lima R B, Ferreira R L C, Silva J A A, et al. 2018. Diameter structure in a community of shrub-tree Caatinga, municipality of Floresta, state of Pernambuco, Brazil. *Revista Floresta*, 48(1): 133–142.

Lopes J F B, Andrade E M, Pereira E C B, et al. 2020. Cut cycles and soil carbon potential stocks in a managed forest in the Caatinga domain in Brazil. *Revista Caatinga*, 33(3): 735–745.

Maia V A, Souza C R, Aguiar-Campos N, et al. 2020. Interactions between climate and soil shape tree community assembly and above-ground woody biomass of tropical dry forests. *Forest Ecology and Management*, 474: 118348, doi: 10.1016/j.foreco.2020.118348.

Malhi R K M, Anand A, Srivastava P K, et al. 2021. Synergistic evaluation of Sentinel 1 and 2 for biomass estimation in a tropical forest of India. *Advances in Space Research*, 69(4): 1752–1767.

Mayamanikandan T, Reddy S, Fararoda R, et al. 2020. Quantifying the influence of plot-level uncertainty in above ground biomass up scaling using remote sensing data in central Indian dry deciduous forest. *Geocarto International*, 37(12).

Menezes R S C, Sales A T, Primo D C, et al. 2021. Soil and vegetation carbon stocks after land-use changes in a seasonally dry tropical forest. *Geoderma*, 390: 114943, doi: 10.1016/j.geoderma.2021.114943.

Mitchard E A T, Saatchi S S, Woodhouse I H, et al. 2009. Using satellite radar backscatter to predict above-ground woody biomass: A consistent relationship across four different African landscapes. *Geophysical Research Letters*, 36(23): L23401, doi: 10.1029/2009GL040692.

MMA (Ministry of the Environment). 2018. Sergipe National Forest Inventory: Main Results. Brasilia: Brazilian Forest Service, 87. (in Portuguese)

MMA (Ministry of the Environment). 2021. Caatinga Biomes. [2021-06-03]. https://antigommagovbr/biomas/caatingahtml. (in Portuguese)

Nascimento Neto J H, Holanda A C, Abreu J C. 2020. Assessing the feasibility of the BDQ method for the sustainable management of the Caatinga. *Revista Caatinga*, 33(3): 746–756.

Nasirzadehdizaji R, Sanli F B, Abdikan S, et al. 2019. Sensitivity analysis of multi-temporal Sentinel-1 SAR parameters to crop height and canopy coverage. *Applied Sciences*, 9(4): 655, doi: 10.3390/app9040655.

Navarro J A, Algeet N, Fernández-Landa A, et al. 2019. Integration of UAV, Sentinel-1, and Sentinel-2 data for mangrove plantation aboveground biomass monitoring in Senegal. *Remote Sensing*, 11(1): 77, doi: 10.3390/rs11010077.

Nguyen L V, Tateishi R, Nguyen H T, et al. 2016. Estimation of tropical forest structural characteristics using ALOS-2 SAR data. *Advances in Remote Sensing*, 5(2): 131–144.

Nóbrega R S, Santiago G A C F, Soares D B. 2016. Trends in oceanic climate control under temporal variability of precipitation in Northeast Brazil. *Brazilian Journal of Climatology*, 18: 276–292. (in Portuguese)

Nuthammachot N, Askar A, Stratoulias D, et al. 2022. Combined use of Sentinel-1 and Sentinel-2 data for improving above-ground biomass estimation. *Geocarto International*, 37(2): 366–376.

Oliveira C P, Ferreira R L C, Silva J A A, et al. 2021. Modeling and spatialization of biomass and carbon stock using LiDAR metrics in tropical dry forest, Brazil. *Forests*, 12(4): 473, doi: 10.3390/f12040473.

Oliveira C P, Ferreira R L C, Silva J A A, et al. 2022. Prediction of biomass in dry tropical forests: An approach on the importance of total height in the development of local and pan-tropical models. *Journal of Sustainable Forestry*, 41(10).

Pereira J E S, Barreto-Garcia P A B, Paula A, et al. 2021. Form quotient in estimating Caatinga tree volume. *Journal of Sustainable Forestry*, 40(5): 508–517.

Periasamy S. 2018. Significance of dual polarimetric synthetic aperture radar in biomass retrieval: An attempt on Sentinel-1. *Remote Sensing of Environment*, 217: 537–549.

Pötzschner F, Baumann M, Gasparri N I, et al. 2022. Ecoregion-wide, multi-sensor biomass mapping highlights a major underestimation of dry forests carbon stocks. *Remote Sensing of Environment*, 269: 112849, doi: 10.1016/j.rse.2021.112849.

R Core Team. 2021. R: A language and environment for statistical computing. Version 4.1.0. R Foundation for Statistical Computing, Vienna, Austria.

Ribeiro A S, Mello A A. 2007. Biota diagnosis. In: Ribeiro A S. *Studies for the Creation of the Grota do Angico Natural Monument*. Sergipe: Secretary of State for the Environment and Water Resources, 12–20. (in Portuguese)

Saatchi S S, Harris N L, Brown S, et al. 2011. Benchmark map of forest carbon stocks in tropical regions across three continents. *Proceedings of the National Academy of Sciences*, 108(24): 9899–9904.

Safari A, Sohrabi H. 2020. Integration of synthetic aperture radar and multi-spectral data for aboveground biomass retrieval in Zagros oak forests, Iran: An attempt on Sentinel imagery. *International Journal of Remote Sensing*, 41(20): 8069–8095.

Salvatierra L H A, Ladle R J, Barbosa H, et al. 2017. Protected areas buffer the Brazilian semi-arid biome from climate change. *Biotropica*, 49(5): 753–760.

Sampaio E V S B, Silva G C. 2005. Biomass equations for Brazilian semiarid Caatinga plants. *Acta Botanica Brasilica*, 19(4).

SEMARH (Secretary of State for the Environment and Water Resources). 2012. Digital Atlas about Water Resources in Sergipe. Sergipe: Sergipe Water Resources Information System, 1–3. (in Portuguese)

Silveira E M O, Terra M C N S, Acerbi-Júnior F W, et al. 2020. Estimating aboveground biomass loss from deforestation in the Savanna and semi-arid biomes of Brazil between 2007 and 2017. In: Suratman M N, Latif Z A, Brunsell N. *Forest Degradation around the World*. London: IntechOpen, 1–17.

Sörensen L. 2007. A spatial analysis approach to the global delineation of dry-land areas of relevance to the CBD. In: *Programme of Work on Dry and Sub-Humid Lands*. Cambridge: UNEP World Conservation Monitoring Centre, 1–8.

Souza D G, Sfair J C, Paula A S, et al. 2019. Multiple drivers of aboveground biomass in a human-modified landscape of the Caatinga dry forest. *Forest Ecology and Management*, 435: 57–65.

Souza M T P, Azevedo G B, Azevedo G T O S, et al. 2020. Growth of native forest species in a mixed stand in the Brazilian Savanna. *Forest Ecology and Management*, 462: 118011, doi: 10.1016/j.foreco.2020.118011.

Tomasella J, Vieira R M S P, Barbosa A A, et al. 2018. Desertification trends in the Northeast of Brazil over the period 2000–2016. *International Journal of Applied Earth Observation and Geoinformation*, 73: 197–206.

Vaghela B, Chirakkal S, Putrevu D, et al. 2021. Modelling above ground biomass of Indian mangrove forest using dual-pol SAR data. *Remote Sensing Applications: Society and Environment*, 21: 100457, doi: 10.1016/j.rsase.2020.100457.

Veloso H P, Rangel-Filho A L R, Lima J C A. 1991. Classification of Brazilian vegetation adapted to a universal system. Rio de Janeiro: IBGE, 123. (in Portuguese)

Vendruscolo J, Marin A M P, Felix E S, et al. 2020. Monitoring desertification in semiarid Brazil: Using the Desertification Degree Index (DDI). *Land Degradation & Development*, 32(2): 684–698.

Vieira R M S P, Tomasella J, Alvalá R C S, et al. 2015. Identifying areas susceptible to desertification in the Brazilian northeast. *Solid Earth*, 6: 347–360.

Vieira R M S P, Sestini M F, Tomasella J, et al. 2020. Characterizing spatio-temporal patterns of social vulnerability to droughts, degradation and desertification in the Brazilian northeast. *Environmental and Sustainability Indicators*, 5: 100016, doi: 10.1016/j.indic.2019.100016.

Vieira R M S P, Tomasella J, Barbosa A A, et al. 2021. Desertification risk assessment in Northeast Brazil: Current trends and future scenarios. *Land Degradation & Development*, 31(1): 224–240.

Wingate V R, Phinn S R, Kuhn N, et al. 2018. Estimating aboveground woody biomass change in Kalahari woodland: Combining field, radar, and optical data sets. *International Journal of Remote Sensing*, 39(2): 577–606.